Magnetically coupled magnet–spring oscillators

2010 Eur. J. Phys. 31 433

(http://iopscience.iop.org/0143-0807/31/3/002)

IOP PUBLISHING EUROPEAN JOURNAL OF PHYSICS

Eur. J. Phys. **31** (2010) 433–452 doi:10.1088/0143-0807/31/3/002

Magnetically coupled magnet–spring oscillators

G Donoso, C L Ladera and P Martín

Departamento de Física, Universidad Simón Bolívar, Apdo. 89000, Caracas 1086, Venezuela

E-mail: clladera@usb.ve and pmartin@usb.ve

Received 11 November 2009, in final form 18 December 2009
Published 10 March 2010
Online at stacks.iop.org/EJP/31/433

Abstract

A system of two magnets hung from two vertical springs and oscillating in the hollows of a pair of coils connected in series is a new, interesting and useful example of coupled oscillators. The electromagnetically coupled oscillations of these oscillators are experimentally and theoretically studied. Its coupling is electromagnetic instead of mechanical, and easily adjustable by the experimenter. The coupling of this new coupled oscillator system is determined by the currents that the magnets induce in two coils connected in series, one to each magnet. It is an interesting case of mechanical oscillators with field-driven coupling, instead of mechanical coupling. Moreover, it is both a coupled and a damped oscillating system that lends itself to a detailed study and presentation of many properties and phenomena of such a system of oscillators. A set of experiments that validates the theoretical model of the oscillators is presented and discussed.

1. Introduction

Ubiquitous in nature and in the man-made world, coupled oscillators are systems that deserve the amount of time that is devoted to them in physics, engineering and mathematics. Their mathematical representations are ideal examples of coupled differential equations to be treated using linear algebra and differential calculus. The familiar coupled oscillator systems are coupled by either linear deformations or torsions of springs, or as in the case of coupled *LC* circuits by magnetic flux. The *canonical* example consists of two pendula horizontally connected with a weak spring whose relaxed length is equal to the distance between the bobs of the pendula [1, 2]. Three aligned mass-points interconnected by two collinear springs is a useful model for studying the longitudinal oscillations of molecules such as CO_2 [1, 3]. Several coupled mechanical oscillators systems, which incorporate magnets and coils, have been recently described. For instance, the oscillations of two nearly identical resonant series *LC* circuits were studied by Hansen *et al* [4]. In that work two nearly identical coaxial coils were placed nearby, one of them was fixed and the other movable along a common axis, and

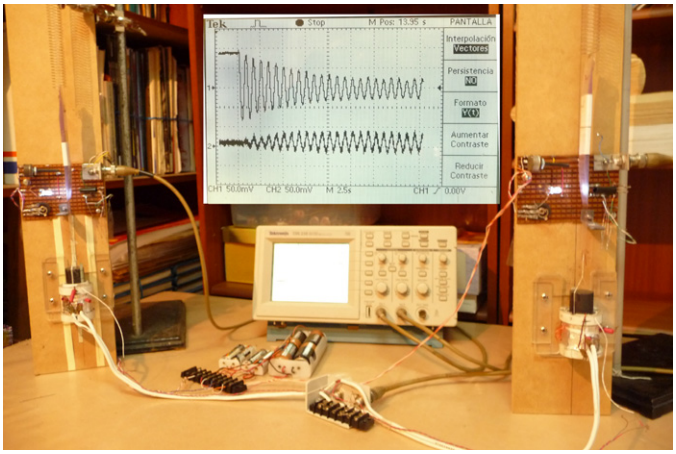

Figure 1. Two ferrite magnets (black cylinders above the white coils, left and right) hang, with same poles down, from two long vertical springs (one on each side) and vertically oscillate in the hollows of the coils. The magnets hanging inside the coils are connected in series, so that the induced currents in them oppose. The oscilloscope screen (inset) shows the magnets' elongations.

(This figure is in colour only in the electronic version)

features of that oscillating system such as the resonance π-phase jumps were studied. Two clamped steel blades, with a strong magnet attached to the free end of each blade, were set in low-frequency coupled oscillations by McCarthy [5]; the oscillations were forced with a driving coil, and a test coil was used to demonstrate effects and concepts such as transients, resonances and the eigen-modes.

Coupled oscillating systems also appear in the quantum world, and some have remarkable properties as in the case of the coupling of the current oscillations of a biased Josephson junction with an external microwave field [6]. At a more sophisticated level, we can mention the coupled electro-magnetic oscillation of two squeezed states of laser beams coherently generated at a nonlinear crystal (optical degenerate parametric oscillator), which is finding important applications in the field of quantum information.

In many mechanically coupled oscillators the variable of the motion equations is either a linear deformation (elongation) or a torsion angle. Here we introduce the new case of two vertical mass-spring oscillators coupled by two electrically conducting coils connected in series (figure 1) not previously found in the literature. An analogous dissipative system of mechanical, in fact torsional, coupled oscillators, is described by Bacon [7] in which the coupling is mechanical, rather than electromagnetic, and provided by a viscous fluid in contact with the oscillators.

In figure 1, the oscillator bobs are two identical magnets oscillating inside, or just above identical coils placed below them, one for each magnet (see also the schematic drawing in figure 5). The magnets induce electro-motive forces in the coils, and the coupling between the two mechanical oscillators is achieved by the electrical current that the motion of the magnets induces in the coils below them. This variable current produces a magnetic force that forces the spring-magnets into oscillation. This new oscillating system is a low-frequency one, and interesting in many senses. To start with, the nature of its coupling is not mechanical but electromagnetic since it is determined by the induced currents in the series circuit. It is a *non-contact* but rather a *field-driven* coupling, a not so common case. Secondly, the relevant

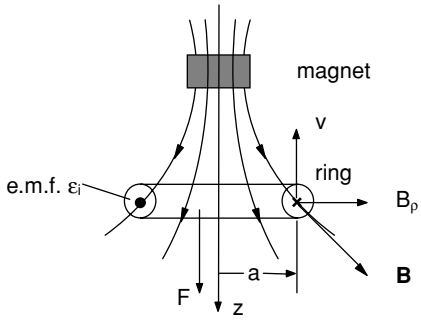

Figure 2. A conducting ring of radius a moves with velocity **v** along the symmetry axis z of the magnetic field **B** of a magnet. The changing magnetic flux induces an e.m.f. ε_i in the ring, and an opposing magnetic force **F** acts on it. B_ρ denotes the radial component of the magnetic field.

variable of the coupling is not a linear or a torsion elongation but instead the speed—the derivative of the elongation variable—of the magnets oscillating in the coils. These features are good arguments to consider this oscillating system for investigation, and as shown below the physics of this oscillating system is ideal for lecture presentation, better yet the system lends itself to an open-ended senior undergraduate laboratory project. Below we present a theoretical model of this new oscillating system and the experiments that validate the model. This work is organized as follows. In section 2 the theoretical model is presented. Section 3 is devoted to the description of the simple experimental setup that allows us to do the necessary experiments and section 4 to the experiments themselves. First we present two preliminary experiments to gather information on the magnitudes of the magnetic force on a magnet oscillating inside a coil, and its dependence with respect to the number of turns in the coil. Then, two cases of the many possible experiments with our electromagnetically coupled oscillators are studied, both theoretically and experimentally. Finally section 5 is devoted to the discussion and conclusions of our model and experiments. Three appendices are given that are devoted to particular features of the two electromagnetically coupled oscillators, and further illustrate their electrical and mechanical properties.

2. Mathematical model of the interaction between a coil and a single oscillating magnet

We begin deriving an expression for the magnetic interaction force between a single magnet and a coil of N-turns. We also need an expression for the electric current in the series circuit of the two coils, the coupling variable. As shown below, a theoretical model for our physical system can be obtained under rather modest assumptions, and taking advantage of the mirror symmetry (figure 1) of the two oscillating spring-magnets. We begin deriving the magnetic force.

2.1. Interaction force between a single-turn coil and a moving magnet

A single conducting loop interacting with a moving magnet is a known problem in electromagnetism [8, 9]. In figure 2 a conducting ring of radius a moves with axial velocity **v** towards a magnet; the changing magnetic flux Φ of the magnetic field **B** induces in this ring an induced

electromotive force (i.e.m.f.) ε_i given by

$$\varepsilon_i = \oint (\mathbf{v} \times \mathbf{B}) \cdot \boldsymbol{dl} = 2\pi a v B_\rho, \tag{1}$$

where v is the speed of the magnet and B_ρ is the radial component of the field at the axial distance z from the magnet. If μ is the magnet *dipole moment*, the radial component B_ρ can be written using the well-known *magnetic dipole approximation* [8, 9] as

$$B_\rho = \frac{3\mu z a}{(a^2 + z^2)^{5/2}}. \tag{2}$$

This simple relation is very convenient for the development of our model (later we will introduce a better approximation, although not so simple, for this radial component of the magnetic field).

If D is the diameter of the conducting ring and σ its electrical conductivity, then the electrical resistance R of the conducting ring is given by

$$R = \frac{2\pi a}{\sigma\left(\frac{\pi}{4}\right) D^2}. \tag{3}$$

We can now write an expression for the magnitude F of the magnetic force acting on the ring at the vertical distance z from the magnet. Such force is (by Newton's third law) the reaction force on the magnet:

$$F = \int i\vec{dl} \times \vec{B} \cdot \hat{z} = i 2\pi a B_\rho = \frac{(2\pi a B_\rho)^2 v}{R}. \tag{4}$$

As expected, because of Faraday's induction law, the force F is proportional to the relative speed v of the ring. After placing B_ρ from equation (2) into equation (4), the magnetic force may be written as

$$F = \frac{36\pi^2 \mu^2 z^2 a^4 v}{(a^2 + z^2)^5 R} \tag{5}$$

for a single-turn coil.

This interaction force is zero for $z = 0$ and it reaches a maximum for the maximum value of the radial component B_ρ of the field. This component may be easily shown to reach a maximum when the conducting ring is at the distance $z = \pm a/2$ from the magnet, and so does the magnetic force F. It may also be inferred from equation (5) that this force rapidly decreases for $z \gg a$, i.e. when the coil is far away from the ring.

2.2. Interaction force between an N-turns coil and a moving magnet

Consider now that we replace the single ring in figure 2 by an N-turns coil of length L. The number of turns in an element of coil of length $\mathrm{d}z$ is $\mathrm{d}N = (N/L)\,\mathrm{d}z$. To find the new expression for the magnetic force exerted on the magnet by this N-turns coil, we use the results for the single-turn coil. We simply need to integrate equation (1) along the z-axis. The induced e.m.f. ε_i generated in the N-turns of wire connected in series is given by the integral (see equation (1) above)

$$\varepsilon_i = \int 2\pi a v B_\rho \,\mathrm{d}N = \int_b^{b+L} 2\pi a \frac{3zav}{(a^2 + z^2)^{5/2}} \frac{N\,\mathrm{d}z}{L}, \tag{6}$$

where b is the distance from the coil top to the mid-plane of the magnet, when at its equilibrium position (figure 3). After integration we get

$$\varepsilon_i = \frac{N}{L}(2\pi a) \left. \frac{(-1)\mu a v}{\left(a^2 + z^2\right)^{3/2}} \right|_{z=b}^{z=b+L}, \tag{7}$$

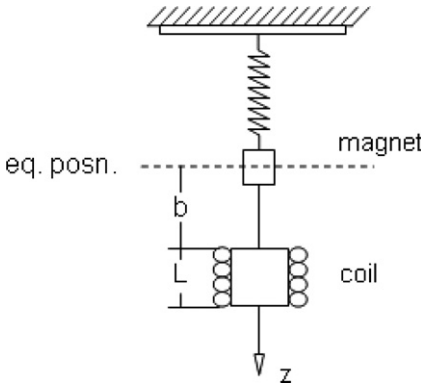

Figure 3. Scheme of a single magnet vertically oscillating in the hollow of a coil. The magnet is shown at its equilibrium position (dashed line). b is the distance from the centre of the magnet to the top of the coil, L is the coil length. The origin of vertical coordinates z is at the centre of the magnet.

which after evaluation at the integration limits gives

$$\varepsilon_i = \frac{N}{L}(2\pi a^2)\mu v \left[\frac{1}{(a^2+b^2)^{3/2}} - \frac{1}{[a^2+(b+L)^2]^{3/2}}\right], \tag{8}$$

which is valid for an N-turns coil.

Using a well-known Faraday expression for the magnetic force (as in equation (4)) between a conductor and a magnet [10], the force dF exerted on the magnet by a coil of infinitesimal length dz carrying a current d$i = (Ni/L)\,\mathrm{d}z$ is given by

$$\mathrm{d}F = \mathrm{d}i\,(2\pi a)\,B_\rho = \left(\frac{Ni}{L}\right)(2\pi a)\,\frac{3\mu a z\,\mathrm{d}z}{\left(a^2+z^2\right)^{5/2}}, \tag{9}$$

which after integration from $z = b$ to $z = b + L$ gives

$$F = \frac{Ni}{L}\,(2\pi a)\,\mu a \left[\frac{1}{(a^2+b^2)^{3/2}} - \frac{1}{[a^2+(b+L)^2]^{3/2}}\right]. \tag{10}$$

Since the total induced current along the N-turns coil is $i = \varepsilon_i/R$, where R denotes the resistance of the coil, we can replace this current i into equation (10) and use equation (8) for ε_i to get the desired expression for the total magnetic force on the N-turns coil:

$$F = \left(\frac{N}{L}2\pi a^2\mu\right)^2 \frac{v}{R}\left[\frac{1}{(a^2+b^2)^{3/2}} - \frac{1}{[a^2+(b+L)^2]^{3/2}}\right]^2, \tag{11}$$

once again valid for an N-turns coil.

Figure 4 is a plot of this magnetic force as a function of the *normalized distance* b/a, for given values of N, a and L, obtained using equation (11). It will be seen that our experiments replicate this theoretical curve with good accuracy.

From equation (11) one might be led to think that the magnetic force between coils and magnets in our set-up (figure 1) increases as N^2. As a matter of fact, this is not so. First, note that the length L that appears in the denominator of the first factor on the rhs of that equation is given by $L = ND$ (assuming a tightly wound coil of a wire with diameter D) and therefore a factor N cancels in the numerator. Secondly, there is a second factor N in the denominator, it is implicit in the coil total resistance value $R = N(2\pi a)/(\sigma\pi D^2/4)$. Finally, note that the square-bracket factor on the rhs of equation (11) becomes larger as the coil length $L = ND$

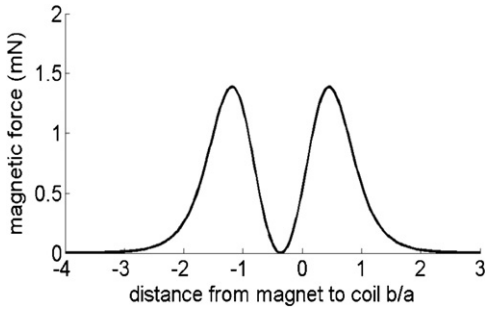

Figure 4. Magnetic force as a function of the normalized axial distance b/a for a coil of $N = 10$ turns and radius $a = 15.0$ mm (plotted for a magnet-to-coil relative speed $v = 0.01$ m s^{-1}). Here the abscissa $b/a = 0$ corresponds to the top of the coil.

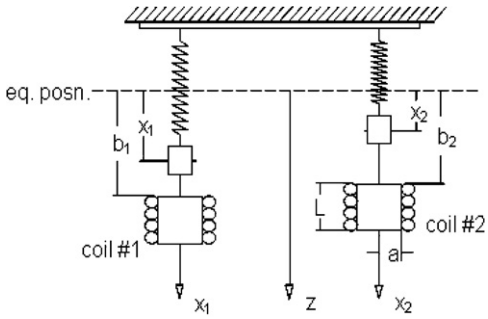

Figure 5. Scheme of the two-coupled-oscillator system. The distances b_1 and b_2 are from the equilibrium position (dashed line) of the magnets to the respective coil, while x_1 and x_2 are the elongations of the mass–spring systems, respectively.

increases and that means a larger force, but the functional dependence on N here is far from being linear, and a more detailed analysis is required (see appendix A).

It is important to study the dependence of the magnetic force upon the number N because intuition usually leads to the suggestion that one would get better coupling by simply increasing the number of turns in the coils, as doing that would increase the linked magnetic flux and therefore the magnetic induction effects. In appendix A we show that for a small number of turns, the force does increases linearly with N, but that a maximum value of the magnetic force is soon reached, and thereafter the magnetic force becomes inversely proportional to N. Therefore, to test our theoretical model it is advisable to set up the experiments with coils of a modest number of turns, say 5–15.

2.3. The coupled oscillations: motion equations

Having dealt with the magnetic force on a single oscillating magnet, we now derive the set of coupled differential equations of the oscillating system. Figure 5 shows the elongation variables $x_1(t)$ and $x_2(t)$ of the oscillating magnets. The coils are at distances b_i with respect to the equilibrium position of the magnets.

Figure 6 shows the equivalent low-frequency electrical circuit of the two coils connected in series, and R_1 and R_2 denote the electrical resistances of coils 1 and 2, respectively.

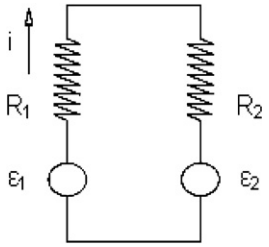

Figure 6. Electric circuit of the coupling coils of the oscillators. R_1 and R_2 denote the electrical resistances of the coils. The coil reactances can be neglected.

We begin the analysis obtaining expressions for the two i.e.m.f.s generated in the circuit by the two moving magnets, namely $\varepsilon_1(t)$ and $\varepsilon_2(t)$ for positions $x_1(t)$ and $x_2(t)$. Applying equation (8), we can write

$$\varepsilon_1(t) = \frac{N}{L}(2\pi a^2)\mu\dot{x}_1\left[\frac{1}{[a^2+(b_1-x_1)^2]^{3/2}} - \frac{1}{[a^2+(b_1-x_1+L)^2]^{3/2}}\right]. \tag{12}$$

A second analogous expression can be written for the i.e.m.f. $\varepsilon_2(t)$ *generated* in the second coil, with the elongation coordinate x_1 and distance b_1 replaced by x_2 and b_2, respectively. The total current in the coils' circuit may be obtained by applying Kirchhoff's laws:

$$i(t) = \frac{\varepsilon_1(t) - \varepsilon_2(t)}{R_1 + R_2}. \tag{13}$$

Assuming now that the elongations of the two magnet-spring systems are relatively small, that is $x_i(t) \ll b_i$, $x_i(t) \ll a$, and assuming identical oscillators (equal masses, equal elastic constants, equal set-up positions $b_i = b$ of the two coils), we may rewrite the coils' current using equation (12):

$$i = \frac{(2\pi a^2)N}{L}\mu\left[\frac{1}{(a^2+b^2)^{3/2}} - \frac{1}{[a^2+(b+L)^2]^{3/2}}\right]\left(\frac{\dot{x}_1 - \dot{x}_2}{R_1+R_2}\right). \tag{14}$$

With the same assumptions of the previous paragraph and using the last equation and equation (11)—already derived for the magnetic force—we may now write the magnetic force opposing the motion of the magnet,

$$F = \left(\frac{N}{L}2\pi a^2\mu\right)^2\left[\frac{1}{(a^2+b^2)^{3/2}} - \frac{1}{[a^2+(b+L)^2]^{3/2}}\right]^2\left(\frac{\dot{x}_1 - \dot{x}_2}{R_1+R_2}\right). \tag{15}$$

If we introduce a constant C (in units of s^{-1}), we may rewrite this force as if it were a *dragging* or *retarding force* acting on the magnet:

$$F = mC(\dot{x}_1 - \dot{x}_2). \tag{16}$$

Using this expression for the magnetic force and applying Newton's second law to the motion of magnet 1, one obtains its motion equation,

$$m\ddot{x}_1 = -kx_1 - mC(\dot{x}_1 - \dot{x}_2); \tag{17}$$

an analogous equation may be written for the motion of the second magnet, and thus we get the set of two coupled differential equations that represents the motion of our two-coupled-oscillator system:

$$\begin{cases} \ddot{x}_1 + C\,\dot{x}_1 + \omega_0^2 x_1 = C\,\dot{x}_2 \\ \ddot{x}_2 + C\,\dot{x}_2 + \omega_0^2 x_2 = C\,\dot{x}_1, \end{cases} \tag{18}$$

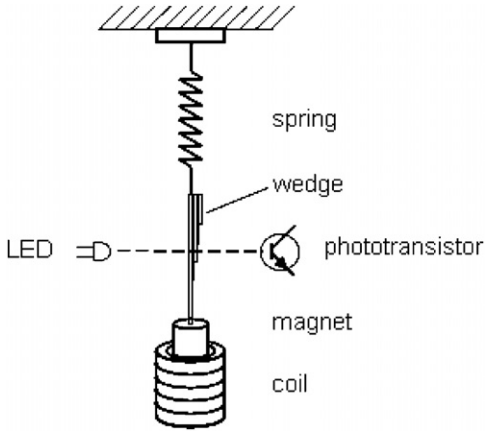

Figure 7. The beam of light from a bright LED traverses a transparent plastic stepped wedge and is then detected by a phototransistor. The wedge, once calibrated, transduces the elongations of the mass-spring into a variable photocurrent.

where the natural angular frequency is given by $\omega_0^2 = k/m$. Equations (18) show that our oscillating system consists of two *damped* harmonic oscillators of natural frequency ω_0, coupled by the electromagnetically induced current in the coils' circuit. A term representing the air drag effects on the oscillators is absent from equations (18) because such effects are in fact negligible (see figure 11).

3. Experiment setup

We set up our system of vertical coupled oscillators (figure 5) using two 55.0 g ferrite cylindrical magnets, 2.20 cm in diameter and 2.54 cm in height, hanging from stainless-steel springs of elastic constant $k = 3.17$ N m^{-1} and 25 mm relaxed length. The upper ends of both springs are attached to a horizontal support. The home-made hollow coils, of a small number N turns of enamelled copper wire of diameter $D = 1.15$ mm, were wrung onto short plastic tubes of radius $a = 15$ mm, and placed just below the magnets. Longitudinal axes of coils and magnets coincide.

A 4 cm long stepped wedge, in fact a stack of about 40 plastic strips (figure 7) cut from a transparency-sheet, was assembled and then placed between the lower end of each spring and the top of the magnet hanging below. For small vertical displacements of the springs, this wedge functions as a variable *optical density light filter* of approximately linear transmittance $T \approx constant \times z$, when placed between a white-light bright LED and a phototransistor.

Figure 7 shows the light beam from the LED illuminating the phototransistor after crossing the lower part of the plastic wedge. When the magnet moves up and down into or nearby the coils, the light beam is modulated by the approximate linear transmittance of the lower portion of the plastic wedge. A digital oscilloscope is used to monitor the photocurrent generated at the phototransistors, and provide digital recordings of the signals. This optical setup is nothing but a *transducer* of the elongation of each mass-spring oscillator into a continuous electrical signal which can be suitably displayed and stored in a digital oscilloscope. An equivalent LED-wedge filter has been described by Greenhow [11]. A commercial linear optical density wedge can also be used at a much higher cost.

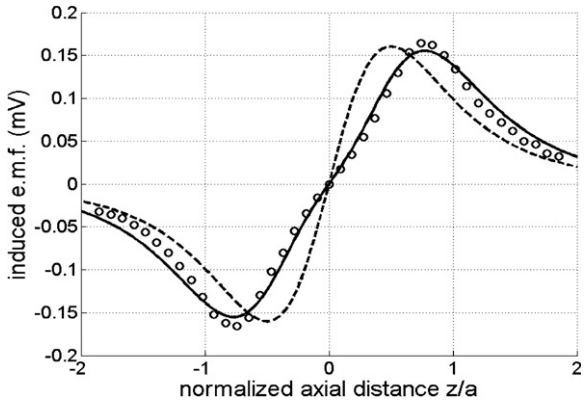

Figure 8. Induced e.m.f. as a function of the normalized axial coordinate. The continuous curve given by the *two-dipole approximation* reproduces the data plotted (circles) with better accuracy than the *single-dipole approximation* (dashes).

It is necessary to adjust the initial position of each magnet—with respect to the nearby coil below—at a set of convenient values, and thus a set of five tiny holes are perforated in a plastic strip that goes between the magnet and the wedge. By inserting a small pin in such holes, one can set the initial amplitudes of the oscillations within a convenient millimetres range.

4. Experimental work

4.1. Magnetic field measurement

To measure the radial component B_ρ of the magnetic field, required in equation (1) for the evaluation of the i.e.m.f.s, we allowed a magnet to fall along the vertical symmetry z-axis of an n-turns *pick-up* coil, of radius a, and measured the i.e.m.f. in that coil as done in a previous work [8]:

$$\varepsilon_i = n2\pi a B_\rho(z) v. \tag{19}$$

Here $z = vt$ and the required speed v is previously measured using a second pick-up coil placed 10 mm below the first [8]. The two transient signals, from the two pick-up coils, are displayed in a scope, and the time interval between them is then used to obtain an accurate value of the speed v. Moreover, the magnetic field is better represented if considered to be the superposition field of *two coaxial magnetic dipoles*, aligned along the *z-axis* and separated by a given distance $2c$. This new parameter c is to be found. Using this two-dipole approximation, we write the component B_ρ as

$$B_\rho = \frac{3}{2}\mu z a \left[\frac{1}{(a + (z - c)^2)^{5/2}} - \frac{1}{(a + (z + c)^2)^{5/2}} \right]. \tag{20}$$

Note that both the magnet dipole moment μ and the new parameter c can be found by simply fitting the experimental curve in our preliminary experiment with the values of B_ρ given by equation (20). In effect, figure 8 shows the experimental values (circles) of the i.e.m.f. generated by the magnet falling along a 20-turn pick-up coil, plotted against the normalized axial distance z/a. Also plotted are the two theoretical curves using the *single-dipole* approximation (*dashed curve*) and the *two-dipole approximation* given by equation (20) (*continuous curve*) for the values $\mu = 3.208 \times 10^{-7}$ T m^3 and $c/a = 0.375$.

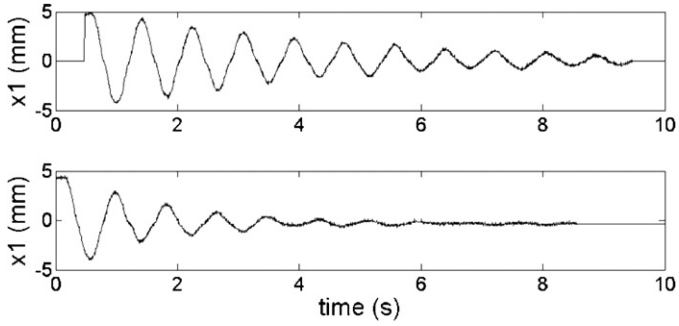

Figure 9. Damped oscillations of a single magnet interacting with a single coil. The curves represent the oscillations $x_1(t)$ of the magnet as a function time: upper curve for the distance $b =$ 18 mm, lower curve for $b = 12$ mm (for a coil of $N = 10$ turns).

Note that the two-dipole approximation is accurate even in the neighbourhood of $z =$ 0; figure 8 shows that only the continuous curve reproduces accurately the position of the maximum and minimum voltages, the width of that maximum and even the inflection point at $z = 0$ of the experimental curve.

4.2. Magnetic force

Using the *two-dipole approximation* we may rewrite our previous equations (8) and (11) for the i.e.m.f. and for the magnet–coil interaction force, respectively, as

$$\varepsilon_{1,N} = \frac{N}{L}(2\pi a^2)\mu v \frac{1}{2}\left[\frac{1}{[a^2+(b-c)^2]^{3/2}} - \frac{1}{[a^2+(b-c+L)^2]^{\frac{3}{2}}} + \frac{1}{[a^2+(b+c)^2]^{3/2}} - \frac{1}{[a^2+(b+c+L)^2]^{3/2}}\right] \tag{21}$$

and

$$F = \left(\frac{N}{L}2\pi a^2\mu\right)^2 \frac{1}{4}\frac{v}{R}\left[\frac{1}{(a+(b-c)^2)^{3/2}} - \frac{1}{[a^2+(b-c+L)^2]^{3/2}} + \frac{1}{(a+(b+c)^2)^{3/2}} - \frac{1}{[a^2+(b+c+L)^2]^{3/2}}\right]^2. \tag{22}$$

Since they are more accurate, these are the expressions we shall be using for the i.e.m.f.s and the magnetic force in what remains of this paper.

Figures 9(a) and (b) are typical experimental plots of the oscillations $x_1(t)$ of a single magnet for two different values of the parameter b. We have also measured the attenuation constant of our coupled oscillators for small oscillations about the equilibrium point of each oscillator. This equilibrium point (figure 5) is located at the distance b from the top of the corresponding coil. The experiments were done for different values of this parameter b and for coils of different numbers, N, of turns. Let n be the order of the decreasing oscillation peaks in the curves of figure 9. The heights of such maxima are given by the following equation:

$$x_n = x\,(nT) = x_0\,\mathrm{e}^{-\frac{C}{2}nT}, \tag{23}$$

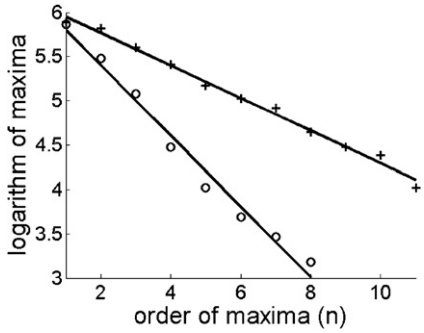

Figure 10. The logarithm of the elongation maxima x_n (mm), of a single oscillating magnet as a function of the order n of such maxima, for $b = 18$ mm (upper straight line) and $b = 12$ mm (lower straight line). The ordinates were calculated using figure 8.

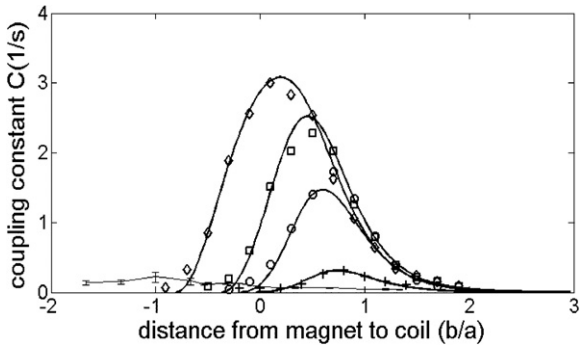

Figure 11. Attenuation constant of the coupled oscillators as a function of the normalized distance b/a for coils of different number of turns, $N = 1$, 5, 10 and 22 (*crosses*, *circles*, *squares* and *diamonds*, respectively). *$b/a = 0$ corresponds to the top of the coil.* The negligible attenuation by air dragging on the magnets is also shown (thin line) with its error bars, plotted with an amplification factor of 10.

where T is the period of the oscillations and C is its *relaxation* or *attenuation* constant. C can then be obtained from the curve. If our theoretical model is correct, this constant C must be the same constant we introduced above in equation (16), in section 2.3, for the dragging magnetic force on our magnets.

Plotting the logarithm of the successive elongation maxima versus their ordinal number n, we can find the *experimental* value of the constant C by fitting a straight line to the experimental points, as has been done in figure 10. The line fitted to the data is given by the equation

$$C = \frac{-2\,(x_n - x_0)}{nT}, \tag{24}$$

where again the x_n is the nth elongation maximum of the magnet and x_0 is the initial amplitude of the oscillations. In figure 11 we show the experimental values of the oscillators attenuation constant C as a function of the normalized distance b/a for coils of different numbers of turns $N = 1$, 5, 10 and 22.

We have plotted in the same figure the theoretical curves (continuous lines) predicted by equations (15) and (16). The curves are plotted from the centre of each coil towards the

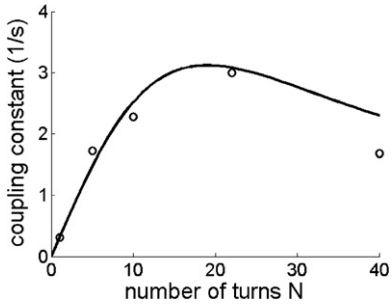

Figure 12. Maxima of the coupling constant (equivalently, the magnetic force) as a function of the number of turns, *N,* of the coils. The force reaches a maximum at about $N = 18$ and then decays for coils with larger numbers of turns. The circles correspond to experimental data.

positive values of the equilibrium position. For the experimental curves plotted in figure 11, the centre of each coil was located at the normalized coordinate $-L/2a = -ND/2a = -0.037$, -0.183, -0.367 and -0807 for $N = 1$, 5, 10, 22, respectively. The curves are symmetrical with respect to such coordinates (see also figure 4 which is the curve for $N = 10$, and the figure in appendix A). Figure 11 also shows the attenuation on the magnets—amplified by a factor of 10—produced by air dragging effects (with the coils in open circuit); the maximum attenuation 0.019 s^{-1} occurs with the magnet completely inside the coil (at $b/a = -1$), a value two orders of magnitude smaller than the attenuation by the Joule effect considered by us.

Figure 12 shows the experimentally obtained maximum values of the coupling constant C as a function of the number of coil turns N (note that the interaction force being proportional to C is also represented in this figure). The plotted points correspond to coils of $N = 1$, 5, 10, 22, and 40. The continuous curve superimposed to the data points has been obtained using equation (22). It may be seen that the maximum of the interaction force grows linearly for a small number of turns, as intuition dictates, but soon the curve reaches a maximum and later decays as N increases, in accordance with our model. The maximum occurs for $N \approx 18$ that corresponds to the parameter $ND/a \approx 1.3$.

In effect, when the number of turns increases, the induced e.m.f. increases too (equation (8)), but the resistance R of the coil also increases with *N,* and this forces the current to decrease. At the same time the total i.e.m.f. is produced only by the very first turns of the coil since the magnetic field of the magnet is of short range. Moreover, the magnet once moving inside a coil produces opposite effects in the loops of wire above and below the coil mid-plane as proved by the anti-symmetrical curve (figure 8) of the i.e.m.f. [8].

4.3. Experiments with the coupled oscillators and their models

The general solution to the linear system of two coupled differential equations (18) is a superposition of a symmetric normal mode of oscillation $x_1(t) = x_2(t) = A\cos(\omega_0 t)$, of angular eigenfrequency ω_0 and an anti-symmetric normal mode represented by $x_1(t) = -x_2(t) = B\,\mathrm{e}^{-Ct}\cos(\omega'_0 t)$, whose eigenfrequency is $\omega'_0 = \sqrt{\omega_0^2 - C^2}$.

Since the electro-magnetic coupling between the two magnet–spring systems is weak, we may consider that the coupling constant fulfils $C \ll \omega_0$, thenceforth $\omega'_0 \cong \omega_0$, and thus the general solution to our system of coupled differential equations is just a linear combination of the following two solutions:

$$x_1(t) = A\cos\omega_0 t + B\,\mathrm{e}^{-Ct}\cos(\omega_0 t) \cong (A + B\,\mathrm{e}^{-Ct})\cos\omega_0 t, \tag{25a}$$

$$x_2(t) = A\cos\omega_0 t - B\,\mathrm{e}^{-Ct}\cos(\omega_0 t) \cong (A - B\,\mathrm{e}^{-Ct})\cos\omega_0 t. \tag{25b}$$

This is the mathematical representation of the elongations of the two magnet–spring oscillators being considered.

Below we analyse two cases of interest of the coupled oscillations of the magnets that may result from varying the initial conditions of motion.

4.3.1. Case I experiment: model and results. At time $t = 0$, magnet 2 will be set at $x_2(0) = 0$, and left there at rest, while magnet 1 will be initially displaced at the vertical position $x_1(0) = 2A$ and then allowed to oscillate. This implies $A = B$, as can be easily checked using equations (25*a*) and (25*b*) above, which become

$$x_1(t) = A(1 + \mathrm{e}^{-Ct})\cos(\omega_0 t), \tag{26a}$$

$$x_2(t) = A(1 - \mathrm{e}^{-Ct})\cos(\omega_0 t). \tag{26b}$$

Each of these two functions is the sum of two harmonic terms: the first of them of constant amplitude A, the second of exponentially decaying amplitude with relaxation, or attenuation, constant C. These equations predict that after a sufficient number of complete oscillations both oscillators' amplitudes should become equal. Then the coupling term becomes zero and the motions of the two magnets are uncoupled:

$$\dot{x}_1(t) = \dot{x}_2(t) \Rightarrow \ddot{x}_1(t) + \omega_0^2 x_1(t) = 0. \tag{27}$$

The two functions in equations (25) are solutions to equations 18(*a*), (*b*) and satisfy the initial conditions for the positions, but only approximately for the initial speeds. Phase differences must be included in the cosine factors in order to exactly satisfy both the position and the speed initial conditions. A more extensive analysis of the solutions can be found in appendix B.

At the beginning of section 3, and in figure 7, we described how to set-up our electromagnetically coupled oscillating system, and explained a technique to determine the elongations of the two oscillating magnets using a LED, a phototransistor and a home-made optical density wedge. The oscillators' parameters used for all the experiments described below are the mass of the magnets $m = 55$ g, spring constant $k = 3.17$ N m^{-1}, period of natural oscillations $T = 0.855$ s and natural angular frequency $\omega_0 = 7.35$ rad s^{-1} (equivalent to a frequency $\approx$1.17 Hz).

Figures 13(a) and (b) show the positions (in mm) of the two magnets as directly read from the oscilloscope screen used to monitor the signals generated by the two phototransistors of the setup. Magnet 1 was initially set in harmonic oscillations from rest with an amplitude $2A =$ 5 mm, while magnet 2 was initially placed at rest at its equilibrium position. The magnet-to-coil equilibrium distance is $b = 17$ mm for both magnets. In the figures we observe the latter oscillating with increasing elongations, while magnet 1 oscillates with decreasing amplitude, until a regime develops in which both magnets oscillate *in phase* with the same amplitude. This happens after both magnets complete about twelve oscillations. The elongations of magnet 1 reduced to $A = 2.5$ mm, i.e. half of its initial amplitude, while magnet 2 elongations grew from zero to the same amplitude A. From $t \approx 13$ s onwards the oscillations of magnet 2 remain of constant amplitude, showing that the air drag on both magnets is negligible.

Small fluctuations in the amplitude of the oscillations of magnet 1 can be noticed in figure 13(a). They are produced by undesirable small lateral oscillations of the magnet, away

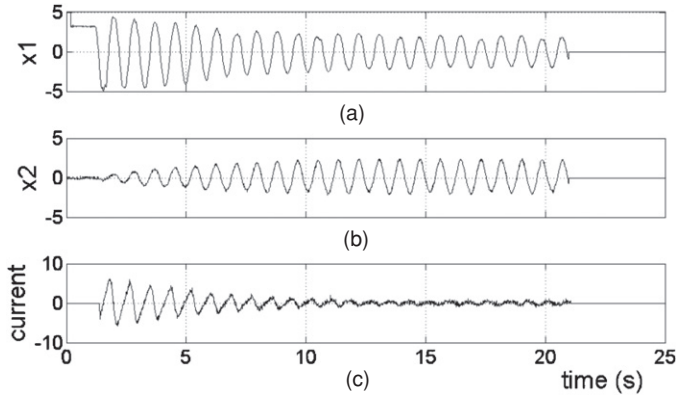

Figure 13. (a) and (b) Elongations (in mm) of the two oscillators as a function of time when magnet 2 starts oscillating from rest at its equilibrium position. (c) Induced current (in arbitrary units) in the coils' circuit as a function of time. After the two oscillators reach the same amplitude, the current becomes negligible.

from the coil axis, which arise from small mechanical perturbations when the magnet is just set into motion at $t = 0$ by the experimenter (the magnet behaves as a conical magnet if one is not careful enough to set it in vertical motion).

Figure 13(c) shows the measured induced electrical current $i(t)$ through the coils. As soon as the two magnets reach equal amplitude oscillations, the current in the coils' circuit fell to zero. As shown in the appendix, the electrical current in the coils' circuit can be represented by (see appendix C)

$$i(t) = -A' \, \mathrm{e}^{-Ct} \sin(\omega_0 t) \,, \tag{28}$$

where

$$A' = 2Aa\omega_0 = 2\sqrt{\frac{mC}{R}}a\omega_0,$$

which shows that the current eventually falls to zero.

According to equation (14) the electrical current in the coils' circuit is proportional to the speed difference of the oscillating magnets. Thus, when magnet 1 begins oscillating it delivers energy to the other oscillating magnet, via the electrical current in the coils circuit, which then increases its elongations. But this transfer of energy is hindered by the heat dissipated in the circuit. The coils' circuit current being dependent upon several of the setup parameters assumes the role of an adjustable coupling.[1]

It may be seen in figure 13 that as soon as the two magnets reach the same maxima of elongations and oscillate in phase (a$t \approx 12T$), the two i.e.m.f.s are, π*-rad,* out of phase and the current present in the coils' circuit become practically zero. The whole oscillating system is then being damped only by the small mechanical air drag on the oscillators, and the system remains in that regime for relatively long time (figure 13(b)). While half of the total initial mechanical energy of magnet 1 is dissipated as heat in the coils circuit (as explained in appendix C), the other half is shared by the two magnets that equate their amplitudes to half of the initial amplitude of magnet 1.

[1] An interesting feature of our coupled oscillators is the adjustable nature of the coupling variable, the electrical current. The latter depends upon the coils' number of turns N, the resistance R of the coils' circuit and the coil-to-magnet distance b. Also, the smaller the distance b the larger the coupling. The coupling could be greatly reduced by simply connecting a resistor in series with the coils.

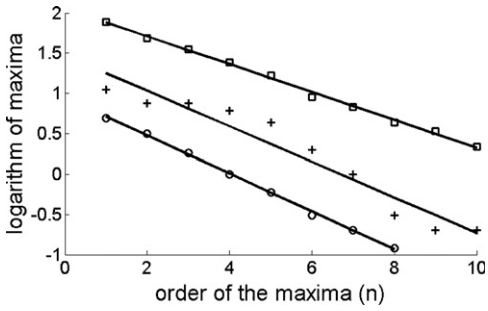

Figure 14. Plot of the logarithm of the exponential term of the elongation maxima of the two magnets in *case I*. The two lower fitted lines correspond to the coupled magnets: *crosses* for magnet 1, *circles* for magnet 2. The upper line shows the logarithm of the maxima of the induced current in the coils.

From figures 13(a) and (b) we obtain the maxima values x_n of the magnet elongations, by simply subtracting the constant amplitude term (see equations (26)). From the additional plot *ln* $(x_n–A)$ versus n shown in figure 14, we then managed to calculate the different coupling constants C for the magnets and the current oscillations (by simply measuring the slopes of the lines plotted).

In figure 14 the two lower lines correspond to the two coupled magnets and from them we have obtained the slope values 0.257 s^{-1} for magnet 1 and 0.275 s^{-1} for magnet 2. The upper line, whose slope is 0.202 s^{-1}, represents the logarithm of the maxima of the induced current. These values are to be compared with the theoretical value of the attenuation constant $C = 0.280\ s^{-1}$ directly obtained using our model (see equations (15), (16) and (22)) for the values $b = 17$ mm and $N = 10$. Note the departures of the elongations of magnet 1 from the fitted straight line. Once again, they are explained by the undesirable lateral oscillations of the magnet inside the coil, as already mentioned above.

4.3.2. Case II experiment: model and results. In the second experiment, the magnets are to be set into oscillations starting from initial coordinates B and $-B$ respectively, simply meaning that $A = 0$ in equations (25*a*) and (25*b*). Then we may write the two magnets' positions as $x_1(t) = B\,\mathrm{e}^{-Ct}\cos\omega_0 t$ and $x_2(t) = -B\,\mathrm{e}^{-Ct}\cos\omega_0 t$, functions that represent two *opposite* damped harmonic oscillators. The magnets will be seen oscillating in perfect synchrony but π*-radian* out of phase. Moreover, as the magnets are set to oscillate with the same amplitude but π-radians out of phase we may write (using equations (18))

$$\dot{x}_1(t) = -\dot{x}_2(t) \Rightarrow \ddot{x}_1(t) + 2C\ \dot{x}_1(t) + \omega_0^2 x_1(t) = 0; \tag{29}$$

that is, both magnets should be seen executing damped harmonic oscillations with a decaying factor $\exp[-2(C/2)t] = \exp[-Ct]$.

Figure 15 shows the actual results obtained for the two magnets oscillating π-radians out of phase. As indicated in *case II* above, both magnets were initially displaced by the same distance B from their equilibrium positions ($b = 13.5$ mm in this experiment), one upwards, the other downwards. In this case, the two i.e.m.f.s in the two coils are initially in phase, and remain so during the magnets' oscillations. Moreover, the coil current is relatively large, and the damping is strong. The magnets come to a halt in a short period of time, and figure 15(c) shows that, as expected, the current soon decays to zero.

From figures 15(a) and (b) we obtained the coordinates x_n of the maxima of the magnet elongations, and from the slopes of additional plots *ln* x_n versus n (not shown) we calculated

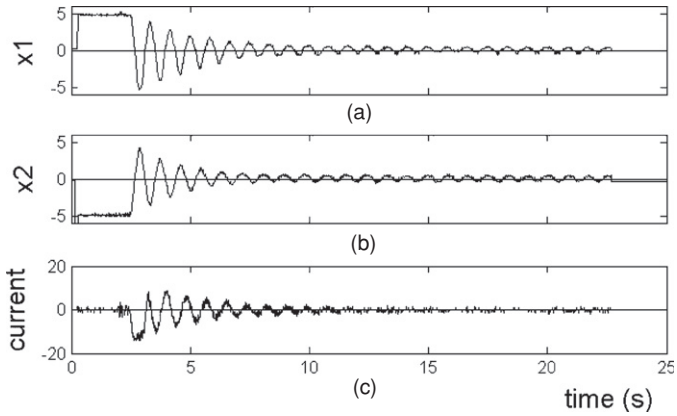

Figure 15. Elongations x_1 and x_2 (in mm) of the oscillators, and the induced current (lower curve) in the coils' circuit as a function of time when the magnets start oscillating π-radians out of phase.

the attenuation new constants C of the magnet oscillations and that of the induced current. The slopes in this second experiment are as follows: 0.380 s^{-1}, 0.420 s^{-1} and 0.309 s^{-1} for the two magnets and the induced current, respectively. The predicted value of C for the present case is 0.404 s^{-1}.

4.4. Measuring the electrical current in the coils' circuit

It is also important to have an idea of the electrical currents induced by the magnet–coil interactions, a variable we cannot directly measure in our experiment. Instead, we measured the induced e.m.f. ε_i in the *open-circuit mode* using a second auxiliary coil of approximately 60 turns wrung onto both setup coils. The electrical current was then calculated simply using its definition $i = \varepsilon_i/R$, where R is the circuit total resistance. The auxiliary coil used was previously calibrated in a separate experiment by comparing with the e.m.f. induced in the main coil, also in the *open-circuit mode*. Note that in our setup the total electrical resistance is $R = R_1 + R_2 + R_{\text{wire}} = 17.2 + 17.2 + 8.0 = 42.4$ m Ω, where R_{wire} is the resistance of the wire connecting the two coils. This total resistance is about 2.5 times the value measured for a single coil. It is interesting to note that the electrical currents that are generated in the coils' circuit are relatively large, of the order of 0.1A in spite of the relatively small induced e.m.f. in the coils by the magnets varying magnetic flux, which are of the order of millivolts.

5. Discussion and conclusions

A pair of magnets vertically oscillating inside hollow magnetic coils connected in series constitutes an interesting new case of coupled oscillators. This system is mechanical but its coupling is electromagnetic, not mechanical. It may be set up with low-cost and modest equipment, readily available in physics laboratories. A set of relations and preliminary experiments have been performed to find the crucial variables of the coupling, namely the induced e.m.f., the induced currents in the coils and the magnetic force between a coil and a magnet. The air drag attenuation on the motion of the magnets was also measured and found negligible. Contrary to intuition the electro-magnetic coupling of our coupled oscillators is not simply directly proportional to the number N of turns in the coils, instead we found a nonlinear dependence upon that number, and that the coupling indeed goes through a maximum as N

varies. We have presented above a successful analytical model for the coupled oscillator system, and performed the experiments to validate the model. A set of two major experiments have been performed to confirm, in a number of ways, the results predicted by the model. In spite of the natural small differences, in the magnet masses, electrical resistance of the coils, different electric dipoles, and the like, our experimental results are of good accuracy. As expected, the measured energy losses caused by air drag on the oscillators are negligible. An important result reported in this work is the measured induced electrical current in the two experimental cases considered.

We believe that our system of coupled oscillators can be used, not only as a demonstration experiment but also as a useful undergraduate laboratory project for honours degree students. It provides many opportunities to introduce all the concepts and relations of coupled oscillators, being in addition a coupled and damped system. With this system of coupled oscillators, one can obtain very accurate results. When performing the experiments we found it very important to keep the magnets oscillating along the vertical, as small initial perturbations rapidly develop into transverse coupled oscillations, the magnets becoming conical oscillators. This is to be avoided. Also, care has to be taken in choosing the vertical axes along which the two magnets oscillate sufficiently separated; otherwise, the magnets will interact and drastically perturb the experiments. In our case we chose axes at about 1 m separation. We believe that both the mathematical model and the experiments performed in the present study can be used to introduce physics students to the problem of coupled oscillators subjected to adjustable and weak coupling.

Acknowledgments

This work was partially funded by Decanato de Investigaciones, Universidad Simón Bolívar, grants G-22 and G-51.

Appendix A.

We show that when the number of turns N in a coil is small, the magnetic force on a coaxially moving magnet, with speed v, is proportional to $\boldsymbol{N}$, and when that number is large, the magnetic force is inversely proportional to that number. There occurs a maximum force when the length L of the coil is approximately equal to its radius a. Let $l = 2\pi\ a$ be the length of a single loop of wire and σ its conductivity. With the variable $u = z/a$, the length of the coil given by $L = ND$, and its electrical resistance by $R = N2\pi a/(\sigma\pi D^2/4)$, our equation (11) for the magnetic force may be conveniently rewritten as

$$F = \frac{\pi^2\mu^2\sigma v}{2Na^3}\left[\frac{1}{(1+u^2)^{3/2}} - \frac{1}{\left[1+\left(u+\frac{ND}{a}\right)^2\right]^{3/2}}\right]^2. \tag{A.1}$$

This force appears plotted in figure A1 for different values of $N = 1, 3, 5, \ldots, 39$, evaluated for a typical magnet maximum speed $v = 0.01$ m s^{-1}. The curves in that figure have been traced from infinite distance above the coil up to the coil centre.

When the number of turns N is small (say 1–10), we have $ND/a \ll 1$ and the square bracket in the *denominator* on the rhs of equation (A.1) may be expanded as

$$\frac{1}{\left[1+\left(u+\frac{ND}{a}\right)^2\right]^{\frac{3}{2}}} \approx \frac{1}{\left[1+u^2+\frac{2uND}{a}\right]^{\frac{3}{2}}} = \cdots = \frac{1}{(1+u^2)^{3/2}}\left[1+\frac{2uND}{a(1+u^2)}\right]^{-3/2}$$
$$= \frac{1}{(1+u^2)^{3/2}}\left[1-\frac{3uND}{a(1+u^2)}\right]. \tag{A.2}$$

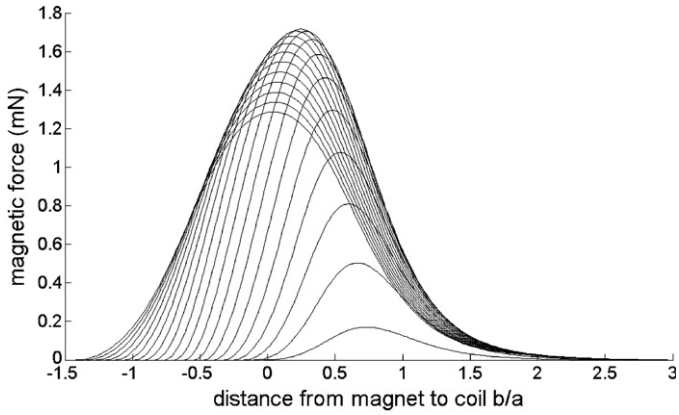

Figure A1. Magnetic force as a function of the *magnet-to-coil* distance . The distance b is measured from the top of the coil to the magnet; a is the coil radius. The curves have been plotted for $N = 1, 3, 5, \ldots, 39$ (lower curve corresponds to $N = 1$).

Replacing this result in equation (A.1) we get

$$F = \frac{\pi^2\mu^2\sigma v}{2Na^3(1+u^2)^3}\left[\frac{3uND}{a(1+u^2)}\right]^2 = \frac{9\pi^2\mu^2\sigma v u^2 N D^2}{2a^5(1+u^2)^5}, \tag{A.3}$$

which shows that the magnetic force is certainly proportional to N when N is small. Furthermore, note that for $N = 1$, the last expression is the same as equation (5), already derived for a single turn in section 2.1. When N is large (say $N > 20$), the second term in the square bracket of (A.1) may be neglected, and the magnetic force decreases with the number of turns, this is expected since the resistance of the coil is then large. A straightforward, yet lengthy, calculation shows that the magnetic force does indeed reach a maximum for $(ND/a) \cong 1.3$, and this is exactly what our experimental results show (figure 12). Note that in the main text we have chosen to plot the coupling constant C instead of the magnetic interaction force. These two are related by $C = F/mv$. In our experiments the product mv is $0.055\ \mathrm{kg} \times 0.01\ \mathrm{m\ s^{-1}} = 0.55 \times 10^{-3}\ \mathrm{kg\ m\ s^{-1}}$.

Appendix B.

Here we show that our equations (25) above give an adequate approximation for the initial conditions of the experiments described in case I and case II. The most general way of expressing the actual positions $x_1(t)$ and $x_2(t)$ of the two oscillators is

$$x_1(t) = A\cos(\omega_0 \mathrm{t} + \delta) + B\,\mathrm{e}^{-Ct}\cos(\omega'_0 \mathrm{t} + \delta'), \tag{B.1}$$

$$x_2(t) = A\cos(\omega_0 \mathrm{t} + \delta) - B\,\mathrm{e}^{-Ct}\cos(\omega'_0 \mathrm{t} + \delta'), \tag{B.2}$$

which after taking derivatives gives the speeds of the two oscillators,

$$\dot{x}_1(t) = -\omega_0 A\sin(\omega_0 t + \delta) - \omega'_0 B\,\mathrm{e}^{-Ct}\sin(\omega'_0 t + \delta') - CB\,\mathrm{e}^{-Ct}\cos(\omega'_0 \mathrm{t} + \delta'), \tag{B.3}$$

$$\dot{x}_2(t) = -\omega_0 A\sin(\omega_0 t + \delta) + \omega'_0 B\,\mathrm{e}^{-Ct}\sin(\omega'_0 t + \delta') + CB\,\mathrm{e}^{-Ct}\cos(\omega'_0 t + \delta'). \tag{B.4}$$

Note that we have introduced four unknown coefficients A, B, δ and δ' which have to be found from the initial conditions.

Fortunately for $t = 0$, we get,

$$x_1(0) = \Delta = A\cos\delta + B\cos\delta', \tag{B.5}$$

$$x_2(0) = 0 = A\cos\delta - B\cos\delta', \tag{B.6}$$

and

$$-\dot{x}_1(0) = 0 = \omega_0 A\sin\delta + \omega'_0 B\sin\delta' + CB\cos\delta', \tag{B.7}$$

$$-\dot{x}_1(0) = 0 = \omega_0 A\sin\delta + \omega'_0 B\sin\delta' + CB\cos\delta'. \tag{B.8}$$

Solving the linear system of these four equations, we get,

$$\tan\delta = 0, \qquad \tan\delta' = -\frac{C}{\omega'_0}, \tag{B.9}$$

$$A = \frac{\Delta}{2}, \qquad B = \frac{\Delta}{2\cos\delta'} = \frac{\omega_0\Delta}{2\omega'_0}. \tag{B.10}$$

Finally, since the damping constant $C \sim 0.257$ is much less than $\omega' \approx \omega_0 = 7.35$ rad s^{-1} (see the case I experiment), the actual values of the phase constants are truly negligible, namely $\delta = 0$ and $\delta' = -2^\circ$, we have $A = B = \Delta/2$ leading to equation (25) in the main text.

Appendix C. Energy conservation applied to the coupled oscillators

We show that, for the oscillations studied in case I, the analytical model of the two coupled oscillators satisfies the conservation of energy (the other case can be treated analogously). We evaluate the amount of energy dissipated as heat by the two coil resistances, and compare it with the difference of energy lost by the mechanical oscillators.

In case I magnet 1 begins its oscillations with amplitude $2A$, while magnet 2 starts from rest at the equilibrium position. Then the initial total energy E_i may be written as

$$E_i = \tfrac{1}{2}k(2A)^2 + 0 = 2kA^2, \tag{C.1}$$

where $k = m\omega_0{}^2$ is the elastic constant of the oscillators springs. The final energy E_f of the oscillators, after about 12 complete oscillations, when both reach the amplitude A is

$$E_f = \tfrac{1}{2}kA^2 + \tfrac{1}{2}kA^2 = kA^2. \tag{C.2}$$

Therefore, the mechanical energy change ΔE in the mechanical system is

$$\Delta E = E_f - E_i = -kA^2, \tag{C.3}$$

which is expected to be equal to the energy dissipated as an amount of heat Q, in the coils' circuit. Let us therefore evaluate the heat Q. The induced current in the coils' circuit is given by equation (14), and may be rewritten in terms of our constant attenuation C introduced in equations (16) and (17) as

$$i(t) = \sqrt{\frac{mC}{R_1 + R_2}}(\dot{x}_1 - \dot{x}_2) = C'(\dot{x}_1 - \dot{x}_2), \tag{C.4}$$

where the constant C is given by

$$C = \frac{(2\pi a^2)N\mu}{L(R_1 + R_2)}\left[\frac{1}{(a^2 + b^2)^{3/2}} - \frac{1}{[a^2 + (b + L)^2]^{3/2}}\right], \tag{C.5}$$

and C' is given by

$$C' = \sqrt{\frac{mC}{R_1 + R_2}}. \tag{C.6}$$

The elongations of the two oscillating magnets in case I are given by (26*a*) and (26*b*), which after differentiation and considering that $C \ll \omega_0$ give

$$(\dot{x}_1 - \dot{x}_2) = -2\omega_0 A\, \mathrm{e}^{-Ct} \sin(\omega_0 t), \tag{C.7}$$

and therefore,

$$i(t) = -2\omega_0 C' A\, \mathrm{e}^{-Ct} \sin(\omega_0 t). \tag{C.8}$$

The total heat dissipated at the two coils is then

$$Q = \int_0^\infty (R_1 + R_2) i^2\, \mathrm{d}t, \tag{C.9}$$

or

$$Q = (R_1 + R_2)(-2\omega_0 C' A)^2 \int_0^\infty \mathrm{e}^{-Ct} \left(\sin(\omega_0 t)\right)^2\, \mathrm{d}t. \tag{C.10}$$

The integral on the rhs gives

$$\int_0^\infty \mathrm{e}^{-Ct} (\sin(\omega_0 t))^2\, \mathrm{d}t = \frac{1}{4\mathrm{C}} - \frac{1}{4\left(\omega_0^2 + \mathrm{C}^2\right)} \cong \frac{1}{4\mathrm{C}}. \tag{C.11}$$

The expression for the heat Q then simplifies to

$$Q = m\omega_0^2 A^2 = kA^2, \tag{C.12}$$

which is exactly the amount of mechanical energy ΔE lost by the oscillators, found above (equation (C.3)).

References

[1] French A P 1971 *Waves and Vibrations* (London: Thomas Nelson) pp 121–57
[2] Crawford F S 1968 *Waves, The Berkeley Physics Course* (New York: McGraw-Hill) pp 116–24
[3] Pain H J 1993 *The Physics of Vibrations and Waves* 4th edn (Chichester, UK: Wiley) p 80
[4] Hansen G, Harang O and Armstrong R J 1996 Coupled oscillators: a laboratory experiment *Am. J. Phys.* **64** 656–60
[5] McCarthy L 2003 On coupled mechanical harmonic oscillators, transients and isolated oscillating systems *Am. J. Phys.* **71** 590–8
[6] Feynman R 1965 *Lectures on Physics* vol 3 (Reading, MA: Addison-Wesley) pp 14–7
[7] Bacon R H 1959 *The Taylor Manual of Advanced Undergraduate Experiments in Physics* ed T B Brown (Reading, MA: Addison-Wesley) pp 59–63
[8] Donoso G, Ladera C L and Martín P 2009 Magnet fall in a conducting pipe: terminal speed and the thickness of the pipe *Eur. J. Phys.* **30** 855–9
[9] Jackson J D 1975 *Classical Electrodynamics* 2nd edn (New York: Wiley) pp 177–80
[10] Halliday D, Resnick R and Krane K 2004 *Physics for Scientists and Engineers* vol 2 (New York: Wiley) chapter 34
[11] Greenhow R C 1988 A mechanical resonance experiment with fluid dynamics undercurrents *Am. J. Phys.* **56** 352–7